

ESA UNCLASSIFIED - For Official Use



European Space Research
and Technology Centre
Keplerlaan 1
2201 AZ Noordwijk
The Netherlands
T +31 (0)71 565 6565
F +31 (0)71 565 6040
www.esa.int

NewAthena mirror performance

European Space Agency
Agence spatiale européenne



APPROVAL

Title NewAthena mirror performance	
Issue Number 1	Revision Number 0
Author Erik Kuulkers, Ivo Ferreira, Matteo Guainazzi	Date 10/05/2023
Approved By Matteo Guainazzi	Date of Approval 11/05/2023

CHANGE LOG

Reason for change	Issue Nr.	Revision Number	Date
First issue	1	0	11/05/2023

CHANGE RECORD

Issue Number 1	Revision Number 0		
Reason for change	Date	Pages	Paragraph(s)
First issue	11/05/2023	All	All

DISTRIBUTION

Name/Organisational Unit
NewAthena Science Redefinition Team, NewAthena Mission Redefinition Team, X-IFU Principal Investigator, WFI Principal Investigator.



Table of contents:

1	INTRODUCTION	4
2	NEWATHENA MIRROR ASSUMPTIONS	4
3	EFFECTIVE AREA	7
3.1	Coating optimization	7
3.2	Effective area estimates	8
4	POINT SPREAD FUNCTION	10
4.1	X-ray tracing results	10
4.2	Empirical approach	10
5	VIGNETTING	15



1 INTRODUCTION

This document describes the release of mirror performance files to be employed by the NewAthena Science Redefinition Team (SRDT) for their assessment of the science case of the NewAthena. The files described therein constitute preliminary, pre-Phase A assessment of the mirror performance. Their accuracy is estimated to be not better than 10%.

This document and the files therein described are not intended to be distributed outside the SRDT, or outside the teams in the Athena Instrument Consortia that are supporting ESA in the definition of the science case of the mission.

Some of the files described in this document were calculated using SIMPOSiuM (Sironi, G., et al., SPIE 2021, 11822, oOM), an advanced and innovative end-to-end X-ray tracing code developed specifically to predict the performance of the Silicon Pore Optics (SPO) technology on Athena. However, in a few cases products generated with SIMPOSiuM had not undergone yet a validation process adequate for them to be publicly distributed. In these cases, performance resource files were generated using empirical approximations of the X-ray tracing results, based on the predicted performance of the Athena Phase B1 telescope Reference Telescope Design – RTD (ATHENA Study Team, 2020, ESA-ATHENA-ESTEC-PL-DD-0001, Issue 3, Revision 1, 24/11/2020), on X-ray tracing simulations at coarser resolution, or both, as described in the following Sections.

2 NEWATHENA MIRROR ASSUMPTIONS

The assumptions for the NewAthena mirror have evolved with respect to Athena. The changes were driven by a combination of the need to save cost and the evolution of the SPO developments.

[The table below gives an overview on the changes and their rationale:]

Table 1: Overview of mirror changes for NewAthena

Parameter	NewAthena baseline	Athena as per the RTD	Rationale
Number of rows / Number of Mirror Modules (MMs)	13/492	15/600	Cost savings on MM production
Rib pitch SPO plates [mm]	2.44	2.30	Evolution of SPO developments
Membrane thickness [µm]	110	150	Evolution of SPO developments
Wedging SPO plates [primary/secondary]	0/+2	-1/+1	Evolution of SPO developments

Commented [MG1]: @Ivo Ferrein: could you please explain how the area losses were calculated?

Commented [IF2R1]: Done briefly in 2.7



Coating of SPO plates [thickness in nm /roughness in nm]	Rows 1-13:	Rows 1-8: Rows 9-15:	Evolution of SPO developments
	1. Cr[12.5/0.45] 2. Ir[10/0.45] 3. C[8/0.45]	1. Ir [10/0.45] 1. Ir[10/0.45] 2. SiC[4/0.45]	

2.1 Number of rows / Number of Mirror Modules (MMs)

For NewAthena the baseline is a Mirror Assembly Module (MAM) populated with 492 MMs. This would allow cost savings in the order of 10 M€. It is assumed that this would correspond to only populating rows 1-13 and cost savings are achieved by (1) reducing the amount of recurrent SPO plates, (2) reducing the production time, and (3) decreasing some non-recurrent costs such as radius dependent tooling, sets of mandrels, and dies. In principle, it is possible to think of a configuration with 492 MMs that is differently distributed over the aperture (i.e., not completely populated rows 1-13) but there might be an impact in the achievable cost savings.

In this document you can also find performance numbers for an alternative configuration with 15 rows/600 MMs that abides by all other NewAthena assumptions. ESA assumes as baseline is 13 rows/492 MMs configuration.

2.2 Rib pitch

The rib pitch is the most important parameter when trying to increase off-axis effective area. It is important to improve the vignetting function as much as possible (driven by azimuthal vignetting which is affected by plate length). The SPO team (ESA+cosine+contractors) decided to push this parameter as much as possible and agreed to target a baseline with an average rib pitch of 2.44 mm. This slightly increases off-axis effective area (as shown later in Section 5) and on-axis effective area.

Note that this is an average value (and was modelled as such). In practice it will vary from plate type to plate type and will also vary within the same plate as it is advantageous to vary the bonding strength (contact area) along the plate width.

2.3 Membrane thickness

For NewAthena it was decided that we shall consider a membrane thickness of 150 µm, instead of the 110 µm assumed for the RTD of Athena.

During the past 1.5 years it was noticed that, although a thinner membrane helps in decreasing the overall anticlastic effects in the SPO plates, it can also pose additional challenges that may impair HEW optimisation, mainly:

- The bending stiffness of the plate is proportional to the thickness to the forth power. Since it is challenging for the SPO plate manufacturers to control the membrane thickness to better than 10-20 µm, the relative change in stiffness (within a plate and from plate to plate) is much higher in SPO plates targeting 110 µm membrane thickness than 150 µm, which has a detrimental effect in terms of figure errors.

Commented [EK3]: Is this something we want to convey?

Commented [IF4R3]: I would say so. We want the community to push for getting these 10 MEur. Really minor in the overall cost of Athena



- The inter-rib stiffness is impacted as one increases the rib pitch and decreases the membrane thickness. When the inter-rib stiffness decreases below a certain threshold, we start seeing some inter-rib sagging (high spatial frequency figure errors).

Note that *cosine* is now assessing configurations with different membrane thicknesses and tuning the stacking and coating processes for the different membrane thicknesses. We reinforce that the 150 μm thickness is an assumption. The actual choice for membrane thickness may evolve during 2023/2024.

2.4 Wedging SPO plates

For NewAthena it was decided to target a configuration consisting of MMs with SPO plates in the primary stacks with no wedge (0), and with SPO plates in the secondary stack with +2 wedge.

When comparing to the (-1/+1) wedging configuration of *Athena*, the (0/+2) configuration of NewAthena is closer to the optimal (+1/+3) configuration, where all the SPO plates are placed with the adequate grazing angle for their radial position. All the details are explained in the RTD. Being much closer to the optimal configuration, allows to gain effective area on axis and off-axis, as also shown and explained in the RTD.

The (0/+2) configuration is only possible due to the recent introduction of the IBF process to not only control the TTV (Total Thickness Variation) of the wafer but also perform the wedging. With the previous chemical wedging process, it was not possible to perform the +2 wedging for the longer SPO plates (lower rows) due to a limitation of the chemical bath.

2.5 Coating of SPO plates

For NewAthena it was decided to update the baseline coating recipe to a tri-layer of Chromium (Cr), Iridium (Ir) and Carbon (C).

During the past 1.5 years, DTU and *cosine* have demonstrated compatibility of the Carbon overcoating with the SPO production process in terms of resilience to the cleaning process (SC-1), resist lift-off procedure, and thermal annealing. Even though there are still some open points regarding the stability of the coating with time, the SPO team decided to assume Carbon as the baseline overcoating for NewAthena, which brings a performance gain with respect to SiC at lower energies. Iridium remains the coating for the second layer to boost high-energy reflectivity.

Underneath the Iridium layer, a new Chromium layer is added to be able to tune the stress introduced by the other 2 layers, a thickness of 12.5 nm is assumed as the baseline (also for the modelling), but the tuning will have to be done per SPO plate type. The introduction of the Chromium layer provides the additional advantage of bringing another degree of freedom to decrease the gain in meridional curvature during the stacking process (known as the stack-up error).



An optimisation process was performed (modelled) to decide on the coating choice for the different radii which is described in Section 3.1. This led to the choice of keeping the same coating recipe for all 13 rows (this same recipe would also be used for the alternative 15 row configuration).

2.6 Detailed geometry

The detailed geometry was generated by re-running the reference telescope generator (part of the RTD) that calculates the positions of all the corners of all the SPO plates to ensure all the spacing and optical related constraints were met with the new assumptions described above. The new membrane thickness and wedging configuration impacted slightly the geometry of each SPO plate (position and dimensions). Then the file with all the SPO plates positions was loaded into SIMPOSium to have a fully consistent geometry setup. The reader can find this file in [SRDT repository/SPO plates](#). Afterwards a series of optics setup and bundle files were generated which were used for all the simulations. These can be found in [SRDT repository/optics files](#).

2.7 Effective area losses/margins

The raw effective area performance numbers coming from SIMPOSium were corrected to account for losses/margins in the same way done for the RTD (Section 5). Some of the losses were modelled already by the fact that we loaded the detailed geometry into SIMPOSium (described above), but others had to be added on top (coming from the Mission Budgets Document). Roughly, the raw effective area numbers resulting from the SIMPOSium simulations were reduced by 20-25% (depending on energy, interpolated based on the losses in the Mission Budgets Document) to account for all losses/margins. The values reported here already include all these losses/margins, unless otherwise noted.

3 EFFECTIVE AREA

3.1 Coating optimization

Simulations in this subsection were done with SIMPOSium, SPORT version 0.5.20 (with Vagrant and VMware Fusion). To speed up the process considerably, we calculated the effective area for one MM in each row. We used 50000 rays per MM. The total effective area was then determined by multiplying the 1-MM effective area by the number of MMs in a row¹ and summing up all rows. The simulation was done per energy, from 0.1 to 15 keV.

The reflectivity curves were calculated using modified scripts from DTU which call the “Modelling and Analysis and Multilayer films” code (IMD; version 5.04; <http://www.rxollc.com/idl/>). We used two kinds of coating: one layer of 10 nm of Ir and

¹ The number of MMs in a row are 24, 24, 24, 30, 30, 36, 42, 42, 42, 48, 48, 48, 54, 54, 54 for rows 1, 2, 3,...,13, 14, 15, respectively.

another tri-layer of Cr/Ir/C of 12.5/10/8 nm. Reflectivity curves were calculated at 1 eV resolution from 0.1-15 keV at incidence angles from 0.1-3 degrees at 0.01 degree resolution (see Figure 1) or less coarser resolution, where appropriate.

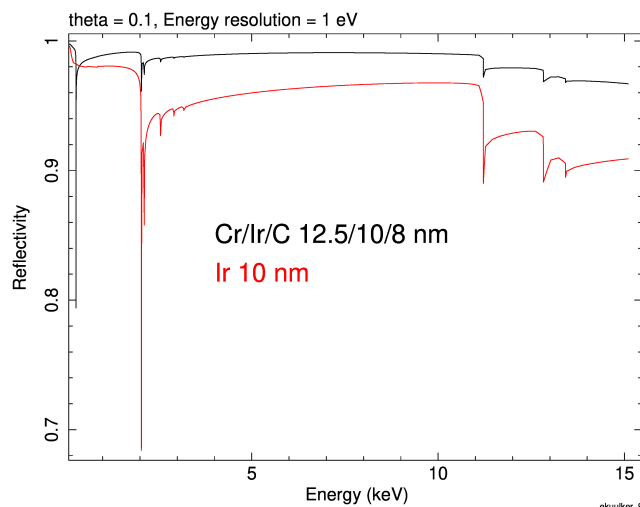


Figure 1 – Reflectivity curves for a single coating layer of Ir with thickness of 10 nm (red) and of a tri-layer of Cr/Ir/C with thickness 12.5/10/8 nm at an incidence angle of 0.1 degrees, with an energy resolution of 1 eV.

One simulation batch was done only Ir as coating on the MMs, and one with only Cr/Ir/C as coating on the MMs. To search for the optimal coating solution we generated effective area curves of a configuration with only Ir coating on all MMs (and so all rows) to a configuration with only Cr/Ir/C on all MMs (and so all rows), i.e., Ir on rows 1-13, 1-12, 1-11, 1-10, ... and Cr/Ir/C on none, row 13, rows 12-13, 11-13, ... etc. For the coating optimization strategy we used reflectivity curves at 100 eV energy resolution and 0.1 degree resolution.

The results for a 13-row configuration are shown in Figure 2 (note that these effective area curves are not corrected yet for area losses, cf. Section 2). A coating of Cr/Ir/C on all rows seems to be best below about 7 keV, while a coating of only Ir on all rows is only slightly better above about 9 keV. Clearly, a solution with a tri-layer coating on all rows is the most effective. For a mirror configuration with 15 rows a similar conclusion can be made, see Figure 3.

3.2 Effective area estimates

Effective area files for both the full mirror 13-row and 15-row configuration at 1 eV resolution over the 0.1 to 3 keV energy range were generated with SIMPOSium version 0.5.23 in a Debian 10 Virtual Machine with 64 Gb of memory. Although they were generated with roughly 5×10^7 rays per keV energy (i.e., 250000 rays per MM), the effective area suffers of

numerical noise at a level of a few percent. This has been removed by applying a smoothing with a boxcar kernel and an energy-dependent width: 30 eV, 10 eV, 60 eV, 25 eV in the energy ranges $E \leq E_{C-K}$, $E_{C-K} < E \leq 0.4$ keV, $0.4 < E \leq E_{IrM5}$, $E_{IrM5} < E < 3$ keV, respectively, where E_{C-K} is the energy of the K_{α} photo absorption edge of Carbon (0.2838 keV) and E_{IrM5} is the energy of the M5 photo absorption edge of Iridium (2.0404 keV). The continuity of the function across the boundaries have been guaranteed by averaging the effective area values across them (difference were never larger than 2%).

In the 3-15 keV energy band, the mirror effective area files as a function of energy at a coarser energy resolution (100 eV) were used (cf. Section 3.1). To create the NewAthena mirror effective area at the required 1 eV resolution, we extrapolated the SIMPOSiuM values using a polynomial function of the second order in the 3 to 10 keV energy range over a 1 eV energy grid. In the 10-15 keV energy range, the X-ray tracing simulations suggest a gradual relative increase of the effective area by $\sim 10\%$ with respect to the *Athena* Phase B1 predictions. However, the statistical quality of the simulated data is still insufficient to make a robust quantitative assessment of this trend. We have therefore conservatively assumed that the effective area follows the same trend as in *Athena*.

The effective area files are available in the [SRDT Teams Group repository](#). The file names are:

- NewAthena_mirror_effectiveArea_IrCCr_13rows_v1.o.dat
- NewAthena_mirror_effectiveArea_IrCCr_15rows_v1.o.dat

for the 13-row and 15-row configuration, respectively. The effective areas are compared in **Error! Reference source not found.**

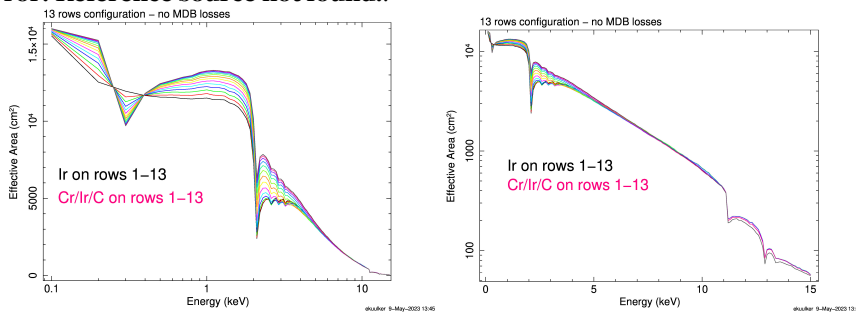


Figure 2 – Effective area curves for different configurations, i.e., from a one-layer coating (Ir) on all rows to a tri-layer coating (Cr/Ir/C) on all rows, see text. At 1 keV, the curve at the bottom has Ir coating on all rows while the top curve has Cr/Ir/C on all rows. All simulations were done at 100 eV energy resolution. The case for a 13-row mirror configuration is shown on a log-lin scale (left panel) and a lin-log scale (right panel).

While we encourage readers to use the official Auxiliary Response Files (ARF) produced by the Instrument Consortia on the basis of the mirror effective areas, correction files that can be applied to the *Athena* Phase B1 effective area files to produce the 13-row and 15-row NewAthena effective areas are also available in the [SRDT Teams Group repository](#). They



should be used for semi-quantitative estimates of the NewAthena performance only. The files names are:

- NewAthena_mirror_AreaCorrFile_IrCCr_13rows_v1.0.dat
- NewAthena_mirror_AreaCorrFile_IrCCr_15rows_v1.0.dat

Prospective users are warned that the current version of these correction files underestimate the effective area at energies $\leq E_{C-K}$ by 10-20%.

4 POINT SPREAD FUNCTION

4.1 X-ray tracing results

X-ray tracing simulation of the Point Spread Function (PSF) based on the latest experimental results at MM level are being generated. They are not available in this release of the NewAthena mirror performance products.

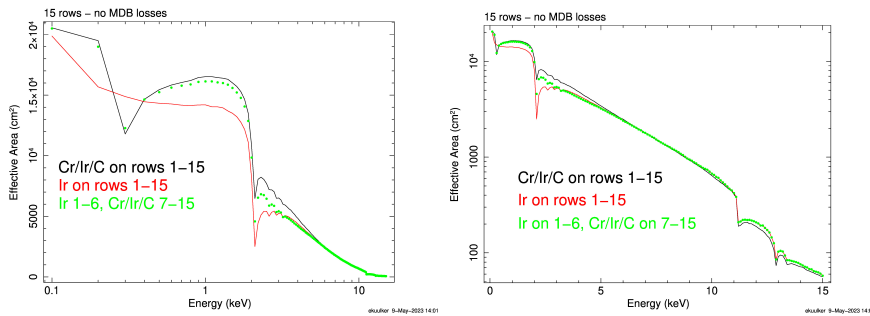


Figure 3 – Effective area curves for 3 different configurations, i.e., Ir on all rows (red), Cr/Ir/C on all rows (black), and Ir on rows 1-6 and Cr/Ir/C on rows 7-15 (dotted green). All simulations were done at 100 eV energy resolution. The case for a 15-row mirror configuration is shown on a log-lin scale (left panel) and a lin-log scale (right panel).

4.2 Empirical approach

PSF analytical approximation as a function of energy² and off-axis angle³ were calculated during the *Athena* Phase B1, based on the experimental results available at that time. They are available in the [SRDT PSF repository](#) for nominal on-axis Half Energy Width (HEW) of

²At the following grid points: 0.2 keV, 0.35 keV, 1 keV, 2.5 keV, 7 keV, and 10 keV.

³At the following grid point: 0, 2, 6, 12, 20, and 28 arcminutes.

5", 6", 7" and 8". They are based on a Voigt function parameterization described in Figure 5 (credit: prof. Richard Willingale, UoL).

For the sake of SRDT simulations, pending the calculation of the PSF with the SIMPOSium ray-tracing simulator (cf. Section **Error! Reference source not found.**), we have extrapolated the parameterization of the *Athena* Phase B1 PSF (corresponding to a mirror structure of 15 rows) to a nominal on-axis HEW=9" (the worst case to be assumed in the SRDT sensitivity analysis)⁴. The parameterization followed these rules:

- α_9 was assumed to be equal to 1
- β_9 was assumed to have the same value as β_8
- FWHM[AB]₉ was linearly extrapolated from the values between FWHM[AB]₆ and FWHM[AB]₈, except for the values corresponding to 10 keV and 28' off-axis angle, for which the FWHM[AB]₈ values were assumed due to limitation in the statistical quality of the fit.

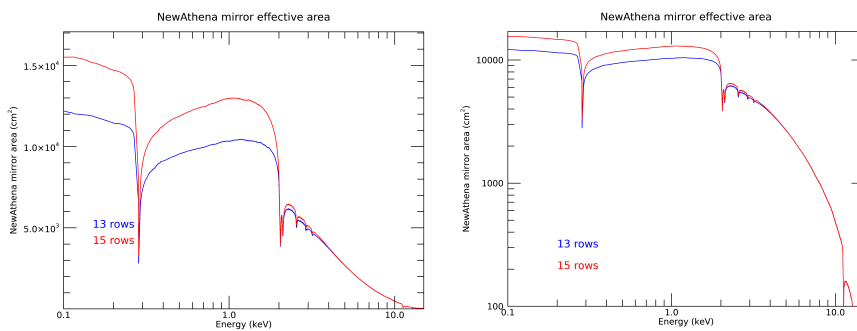


Figure 4 – NewAthena mirror effective areas as a function of energy for the 13-row (blue) and the 15-rows (red) configuration with the y-axis in lines (left panel) and logarithmic scale (right panel).

The extrapolations as a function of energy and off-axis angle are shown in Figure 6. The corresponding images and HEW (calculated by F. Carrera, IFCA) are shown in Figure 7.

⁴In the same directory, a file corresponding to an on-axis HEW of 10" is also available, for comparison with the DARWISH exercise.



Full Aperture PSF

- Ray trace full aperture of 600 modules
- Each module PSF modelled using pseudo-Voigt distribution for in-plane and out-of-plane figure errors (as above)
- Full aperture PSF elliptical - major axis FWHMA in azimuthal direction, minor axis FWHMB in radial direction
- Fit the PSF using a 2-D distribution – radial profile a modified pseudo-Voigt distribution

$$F(r) = (1 - \alpha) \exp\left(\frac{-r^2}{2\sigma_g^2}\right) + \alpha \left(1 + \frac{r^2}{\sigma_c^2}\right)^{-\beta}$$

$$\sigma_g = \frac{FWHM}{2\sqrt{2\ln(2)}}, \sigma_c = \frac{FWHM}{2\sqrt{2^{1/\beta}-1}}$$

$$F(0) = 1$$

- The Cauchy component (Lorentzian) is modified by index β
- Position of source in FOV (x_0, y_0) – origin on-axis - off-axis angle of source $\sqrt{x_0^2 + y_0^2}$
- Position angle of source in FOV $P = \text{atan}(y_0/x_0)$
- Radius from source position $r = \sqrt{(x-x_0)^2 + (y-y_0)^2}$
- Position angle wrt the major axis $q = \text{atan}((y-y_0)/(x-x_0)) + \pi/2 - P$
- Elliptical FWHM = $\sqrt{(FWHMA \cdot \cos(q))^2 + (FWHMB \cdot \sin(q))^2}$

Figure 5 – Description of the PSF parameterization (Credit: prof. Richard Willingale, UoL)

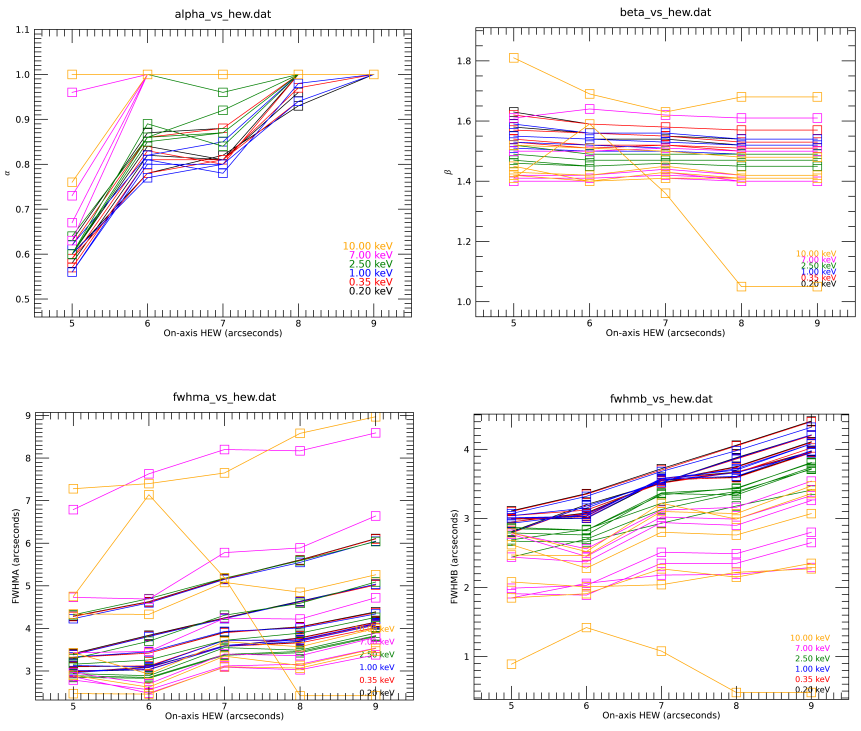


Figure 6 – PSF parameters as a function of on-axis HEW for different energies (labelled) and off-axis angles. Additional plots with off-axis angles labelled are available in the SRDT PSF repository.

PSF file: na_psf_vig_hew_9.dat
 Image width=60.0 arcsec Pixel size=0.50 arcsec
 Red: circular HEW area
 Green: contours including 25% (solid), 50% (dashed), 75% (dot-dashed), 90% (dotted)
 Normalisation file: norm_9_dx0p5_20arcmin.topcat

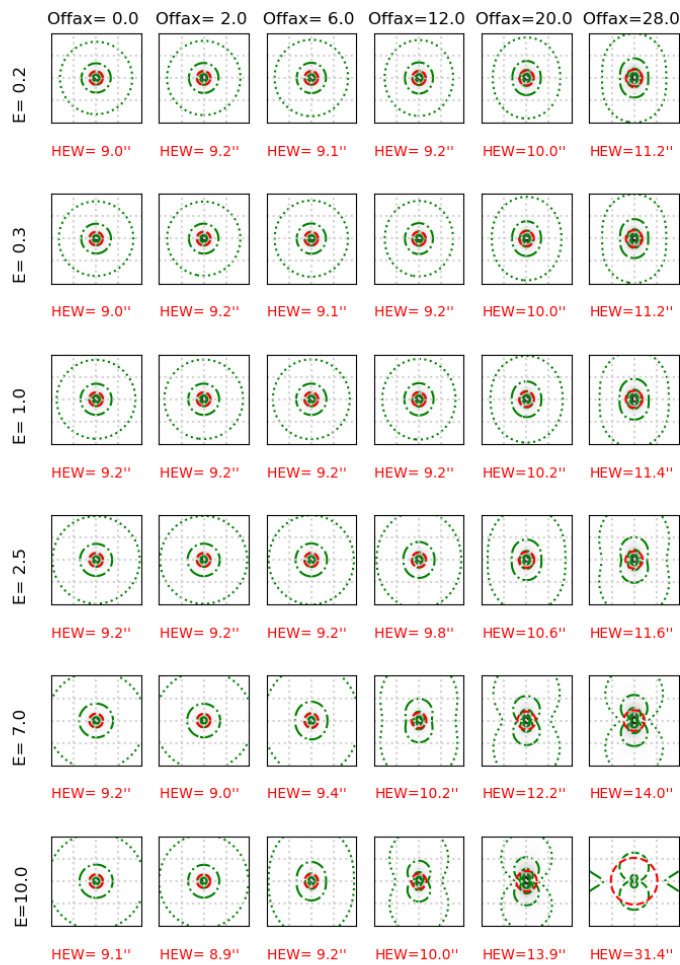


Figure 7 – PSF images and calculated HEW as a function of energy and off-axis angle (calculated by F. Carrera, IFCA). Explanation of curves and color scheme in the header.



5 VIGNETTING

The vignetting function as a function of energy and off-axis angle calculated using SIMPOSiuM for the 13-row and 15-rows configuration is shown in Figure 8. It follows a similar shape to *Athena*, only slightly better due to the larger rib pitch (2.44 mm vs. 2.30 mm). There might also be a benefit due to the wedging (0/+2 vs -1/+1) but it is second order. The raw data is provided in the form of .dat files and an Excel spreadsheet with the values of effective area (A_{eff}) and the graphs in the [SRDT repository/vignetting](#).

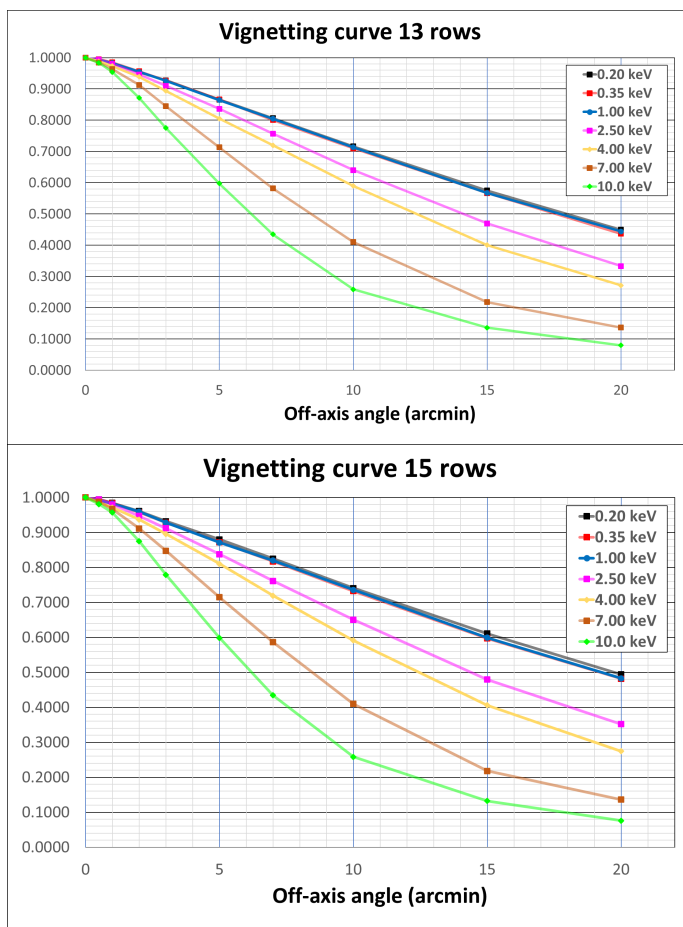


Figure 8 – NewAthena vignetting as a function of energy and off-axis angles for the 13-row (top panel) and 15-row (low panel) configurations.